



STUDY ON THE EFFECT OF NUMBER OF FILM COOLING ROWS ON THE THERMAL PERFORMANCE OF GAS TURBINE BLADE

S. F. SHAKER*, M.Z. ABDULLAH, M. A. MUJEEBU, K.A. AHMAD and M.K. ABDULLAH

School of Mechanical and Aerospace Engineering, Universiti Sains Malaysia, Engineering Campus,
14300 Nibong Tebal, Penang, Malaysia.

*Corresponding Author: Email: sufianfarid@yahoo.com, Phone: 006045996310

(Geliş Tarihi: 17. 01. 2011, Kabul Tarihi: 18. 03. 2011)

Abstract: This paper presents three dimensional (3D) numerical investigations on the effect of film cooling on the thermal behavior of gas turbine blades, using a commercial computational fluid dynamics (CFD) code. The 3D airfoil geometry of the blade which emulates the actual (A-4 Skyhawk) blade is generated in the pre-processor (GAMBIT). Two cooling configurations namely 1) four rows film cooling with U-bend internal channel and 2) eight rows film cooling with U-bend internal channel, have been simulated to be transonic flow over a turbine blade with turbo-specific non-reflecting boundary conditions (NRBCs). Turbulence is represented using the shear-stress transport (SST) model, and the flow is assumed to have a free-stream turbulence intensity of 9%. The heat transfer coefficient, total temperature distribution, static pressure and velocity vector are investigated. The effect of coolant injection pressure ratio ($P_{R,ci}$) on temperature distribution is also investigated. The results show that heat transfer coefficient with film cooling is higher than that without film cooling. From the predicted temperature profile, it is observed that the blade with eight rows film cooling with U-bend internal channel shows better cooling performance than that with four rows. Further, increase in $P_{R,ci}$ leads to reduction in temperature and moreover the lateral spreading facilitated the best coolant layer.

Keywords: Turbine blade; Film cooling; Finite volume method; Temperature distribution; Shear-stress model; Heat transfer coefficient.

GAZ TÜRBİNİ KANATÇIĞININ TERMAL PERFORMANSINA FİLM SOĞUTMA KADEME SAYISININ ETKİSİNİN İNCELENMESİ

Özet: Bu çalışmada, ticari bir hesaplamalı Akışkanlar Dinamiği (HAD) kodu kullanılarak, gaz türbini kanatçıklarının termal davranışına film soğutmanın etkisi üç boyutlu (3D) sayısal olarak incelenmiştir. Gerçek bir A-4 Skyhawk kanatçığının üç boyutlu geometrisi GAMBIT ön-prosesörü ile oluşturulmuştur. İki farklı soğutma konfigürasyonu: 1) U- dirsekli iç kanallı dört sıra film soğutma; 2) U- dirsekli iç kanallı sekiz sıra film soğutma için turbo-spesifik yansıtmasız sınır şartları altında bir türbin kanatçığı üzerindeki transonik akış simule edilmiştir. Türbülans modeli olarak kayma gerilmesi aktarımı (SST) model kullanılmıştır. Akışın serbest-akış türbülans şiddeti 9% kabul edilmiştir. Isı transfer katsayısı, toplam sıcaklık dağılımı, statik basınç ve hız vektörlerinin değişimi incelenmiştir. Sıcaklık dağılımına, soğutma püskürme basınç oranının ($P_{R,ci}$) etkisi de incelenmiştir. Film soğutmalı ısı transfer katsayısının film soğutmasız durumdan daha yüksek olduğu görülmüştür. Sıcaklı profillerinden, U- dirsekli iç kanallı sekiz sıra film soğutmalı kanatçığının U- dirsekli iç kanallı dört sıra film soğutmalı kanatçığa göre daha iyi soğutma performansı sergilediği görülmüştür. Püskürme basınç oranının ($P_{R,ci}$) daha fazla artırılması sıcaklıkta daha fazla düşüşe sebep olmuştur ve ayrıca yanal püskürtmenin en iyi soğutma tabakası oluşturduğu görülmüştür.

Anahtar Kelimeler: Türbin kanatçığı, Film soğutma, Sonlu hacimler metodu, Sıcaklık dağılımı, Kayma gerilmesi aktarımı; Isı transferi katsayısı.

INTRODUCTION

The higher temperatures involved in modern gas turbines necessitate the development of efficient cooling techniques for the blades, without sacrificing the thermal efficiency. In the recent past, many researchers have focused on numerical and experimental investigations on various cooling techniques for gas turbine blades. Of the available methods, film cooling has been proved to be the most efficient technique.

Abuaf et al. (1997) determined both heat transfer coefficient and film cooling effectiveness distributions in a linear airfoil cascade. Heat transfer coefficient and film cooling effectiveness distributions were obtained for a linear airfoil cascade, with and without film coolant injection. Chernobrovkin and Lakshminarayana (1999) introduced a modified viscous flow solver based on the Runge–Kutta scheme for the numerical investigation of the aero-thermal field due to the leading edge film cooling at a compound angle. A three-dimensional Navier–Stokes simulation was performed

by Heidmann et al. (2000) for a realistic film cooled turbine vane using the LeRC-HT code. The simulation included the flow regions inside the coolant plenum and film cooling holes in addition to the external flow. The vane had both circular cross-sectional and shaped film cooling holes and was modeled by using a multi-block grid, which accurately discretized the actual vane geometry including shaped holes. Experimental and numerical investigations of convective heat transfer on the first-stage blade tip surface for a geometry typical of large power generation turbines had been performed by Bunker et al. (2000) and Ameri and Bunker (2000), by using LeRC-HT code. A stationary blade cascade experiment was run consisting of three airfoils, the center airfoil having a variable tip gap clearance. The airfoils were made according to the aerodynamic tip section of a high-pressure turbine blade with inlet Mach number of 0.30; exit Mach number of 0.75, pressure ratio of 1.45, exit Reynolds number based on axial chord of 2.57×10^6 , and total turning of about 110 deg. A hue detection based liquid crystal method was used to obtain the detailed heat transfer coefficient distribution on the blade tip surface for flat, smooth tip surfaces with both sharp and rounded edges. Good comparison with the experimental measured distribution was claimed. Teng et al. (2000) measured the film effectiveness and coolant jet temperature profile on the suction side of a gas turbine blade using a transient liquid crystal and a cold-wire technique, respectively. The blade had only one row of film holes near the gill hole portion on the suction side of the blade. Tests were performed on a five-blade linear cascade in a low-speed wind tunnel. The effect of wake passing on the showerhead film cooling performance of a turbine blade has been investigated experimentally by Heidmann et al. (2001). The flow and heat transfer due to film cooling over a turbine nozzle guide vane, which was also cooled by internal convection, were numerically analyzed under engine conditions, by Sarkar et al. (2001). The transient, two-dimensional, mass-averaged, Navier–Stokes equations were solved in the physical plane based on the four-stage Runge–Kutta algorithm in the finite volume formulation. The experiments were performed in an annular turbine cascade with an upstream rotating row of cylindrical rods. Steady computations were found to be in excellent agreement with experimental Nusselt numbers, but over-predicted the experimental film effectiveness values. The discrepancy was attributed to the inability to match actual hole exit velocity profiles and the absence of a credible turbulence model for film cooling. Heat transfer coefficient and film cooling effectiveness on a gas turbine blade tip were measured by Kwak and Han (2003) using hue detection based transient liquid crystals technique. Tests were performed on a five-bladed linear cascade with blow-down facility. Kwak and Han (2003) measured the detailed heat transfer coefficients and film cooling effectiveness. The test blade had a squealer (recessed) tip with a 4.22% recess. The blade model was equipped with a single row of film cooling holes on the pressure side near the tip region and the tip surface along the camber line. Hue detection

based transient liquid crystals technique was used to measure heat transfer coefficients and film cooling effectiveness. This study was extended by Kwak et al. (2003) and Kwak and Han (2003), to focus on the shroud and near tip regions of the pressure and suction sides. Experiment and computational fluid dynamics (CFD) simulation using finite volume method (FVM) (Fluent Inc, 2002), of heat transfer in trailing edge film cooling in gas turbine blades was presented by Martini et al. (2003).

Ahn et al. (2005) studied the film cooling effectiveness on a gas turbine blade tip using the pressure-sensitive paint (PSP) technique. Air and nitrogen gas were used as the film cooling gases, and the oxygen concentration distribution for each case was measured. In their extended studies, they focused on the leading edge of a rotating gas turbine blade with two rows (2006) and three rows (2007) of holes aligned to the radial axis. PSP has also been used by Gao et al. (2007) to study film cooling with four kinds of hole configurations: cylindrical, laterally-diffused (fan-shape), forward-diffused (laid-back), and laterally- and forward-diffused (laid-back fan-shape). The use of FVM code (Fluent Inc, 2002) has also been reported by Yang et al. (2007) who studied the effectiveness and the heat transfer coefficient in a 1-1/2 turbine stage, with three rows of film cooling holes. Three-dimensional CFD prediction and improvement of holes arrangement of a film cooled turbine blade using a feature-based jet model was presented by Burdet and Abhari. (2007). Choi et al. (2008) concentrated on the cutback trailing edge of a turbine blade with slot ejection, using the liquid crystal technique. Another PSP based study has recently been made by Gao et al. (2009) who used compound angle laidback fan-shaped holes to cool the blade surface with four rows on the pressure side and two rows on the suction side. Very recently, the suitability of three different two-equation turbulence models; $k-\epsilon$ model, the $k-\omega$ model and the shear stress transport $k-\omega$ model, in predicting film cooling effectiveness on a rotating blade was investigated by Tao et al. (2009). To fulfill this target, both numerical simulation and the experimental investigation were carried out for a rotating blade. The standard $k-\epsilon$ model was shown to be the poorest in prediction. Few of the remaining works include those of Yang et al. (2009), Scheepers and Morris (2009), and Montomoli et al. (2009).

While going through the previous studies, it becomes obvious that many researchers have studied the film cooling both numerically and experimentally. However, the use of FVM-based commercial CFD (Fluent Inc, 2002) code which is appreciably cheaper than the codes used by most of the previous workers, has rarely been reported (Martini et al., 2003, Yang et al., 2007). In the current study, the work of Yang et al. (2007) is extended for different turbine blade geometry, blade material, number of cooling rows and operating conditions. The standard (27) blade model of AL 6XN ® stainless steel alloy is considered. The shear-stress transport (SST) model (Menter, 1994) is used in this work since Tao et al. (2009) reported that the standard $k-\epsilon$ model gave

worse prediction. Another contribution of the present work is the treatment of the problem with turbo-specific non-reflecting boundary conditions (NRBCs). Four and eight rows of cooling holes are separately studied at a maximum working temperature of 1700 K. The temperature, pressure and velocity distributions, and the heat transfer coefficient in each case are observed and compared, in order to find out the better configuration.

THE PHYSICAL MODEL

Figure 1 shows the geometry of the blade with various configurations of blade models. Figures 1 (a) and (b) consider the combination of internal and external cooling. In Figure 1 (a) there are four rows of film

cooling holes, two at the suction side (SS) and two at the pressure side (PS). Each row has a number of film cooling holes, the distance between them (p) is 2.388 mm in the span-wise direction and the diameter (d) is 0.4 mm, so that the ratio, $p/d = 5.97$. In Figure 1 (b) there are eight rows three at the suction side, three at the pressure side and two at the leading edge. The specifications and the aerofoil shape are similar to the standard (27) blade with the same scale. The diameter of the circular section plenum channel is 2.5 mm. It may be noted that most of the previous researchers focused on the blade tip; the present study focuses on the blade surface, suction and pressure sides. In this work, the tip clearance is not included, rather the percentage of span-wise sectioning is considered.

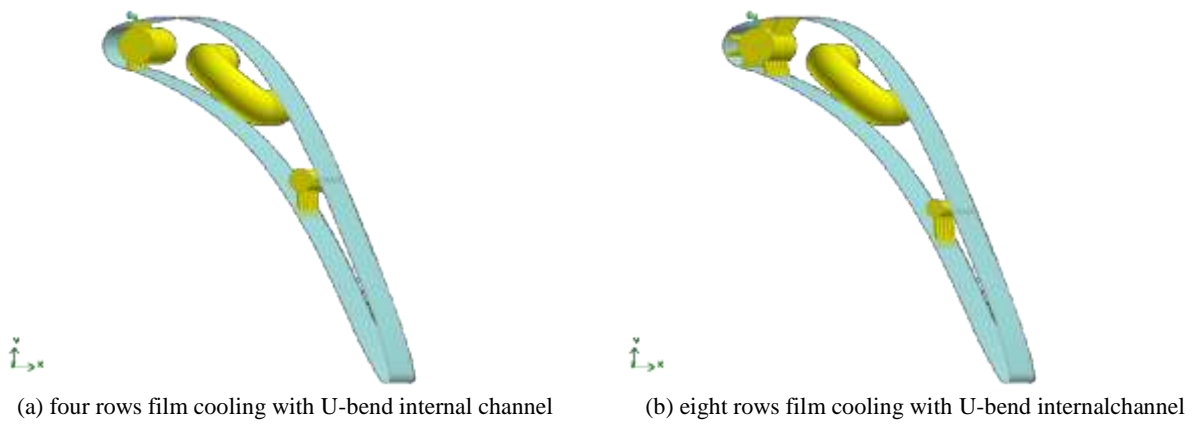


Figure 1. The 3-D blade models showing the cooling configurations.

THE NUMERICAL SIMULATION AND PROCEDURE

This study presents the simulation of transonic flow over a turbine blade with turbo-specific non-reflecting boundary conditions (NRBCs). The standard pressure boundary conditions for compressible flow fix specific flow variables at the boundary (e.g., static pressure at the outlet boundary). As a result, the pressure waves that incident on the boundary will reflect in an unphysical manner, leading to local errors. The effects are more pronounced for internal flow problems where boundaries are usually close to geometry inside the domain, such as compressor or turbine blade rows. The present case considers the transonic flow around a turbine blade cascade with a shortened exit boundary. This configuration is frequently encountered in stage analyses where the spacing between adjacent blade rows is small, and hence, the exit boundary of the upstream row must be placed very close to the trailing edge of the blade. The traditional pressure outlet boundary treatment can lead to spurious pressure distributions on the blade surface since the exit pressure is typically assumed to be uniform in the blade-to-blade direction. NRBCs can eliminate this problem by permitting pressure waves to pass through the boundary without reflection, thereby leading to a more accurate solution. It is worth noting that the NRBCs can only be used with density-based solver. The gas turbine blade geometry is

generated by the GAMBIT pre-processor. GAMBIT code is used to generate the unstructured grids, with grid clustering inside the blade boundary layer and the film cooling region. Triangle Pave mesh, an automatic multiblock grid generator was used to generate the grids. Triangle Pave mesh produces grids with unstructured, smooth, and T- grid hybrid elements throughout the volumetric region. The advantage of T-grid hybrid elements is that it can be used in a complex geometry such as blade. Clustering of the grid in this case is done on the blade surfaces, circular plenum and film cooling tubes. The solid domain is applied to the turbine blade and the rest is declared as fluid. The unstructured Triangle Pave mesh is used for both of the blade models. The number of cells depends on the geometry of the turbine blade, circular plenum and the number of film cooled holes. The blade with four rows film cooling and eight rows film cooling uses cells of 380138 and 405564 respectively. The blade span for the two models is 15% of the height (H). The scaled up blade has a constant axial chord length of 31 mm, and the span is 100 mm the blade leading edge pitch is 31 mm. The blade channel diameter is 2.5mm and the diameter of the channel that located at the first third of blade is 1.5mm. The assumptions in 3-D computational model include turbulent, compressible flow with no buoyancy or radiation contributions.

Figure 2 represents the periodic boundary condition setup for the blade. The volume is divided into two domains. First is solid for the blade and second is fluid for gas region. The entrance surface for air declared as pressure inlet and the rear surface is pressure outlet. The blade passage consists of one blade without clearance and two shaped walls representing the adjacent blades. The flow is set as turbulent and steady with inlet Reynolds number 1600000, and energy model is enabled to solve the energy equation. The gas temperature is set as 1700 K and high atmosphere pressure is considered. The second order upwind scheme is used for solving momentum and energy equations, and the ‘simple’ method is selected for pressure-velocity coupling. The criteria of convergence are set as 1×10^{-3} for continuity, and 1×10^{-5} for velocities in x and y axes, and for energy. The simulation took about 96 hours in a Pentium (R) 4 (CPU 2.20GHz, 2.00GB RAM) processor.

RESULTS AND DISCUSSION

Mesh sensitivity

The initial task was to establish the mesh size so that the results obtained are grid independent. In the present study, the gas turbine blade models are checked with two different numbers of meshes such as 505162 and 405564. In the case of eight rows film cooling, it has been observed that the highest percentage difference in temperatures between the two cases is only 0.8% or 0.5K. Hence the modeling with mesh number of 405564 cells is found sufficient for the present study.

Model validation

The present simulation results of heat transfer coefficient and pressure flow around the aerofoil surface are compared with those obtained by Bunker et al. (2000) and Ameri and Bunker (2000). The comparison is shown in Figures 3 and 4 respectively. The figures show that the present predictions are in par with the previous numerical and experimental values.

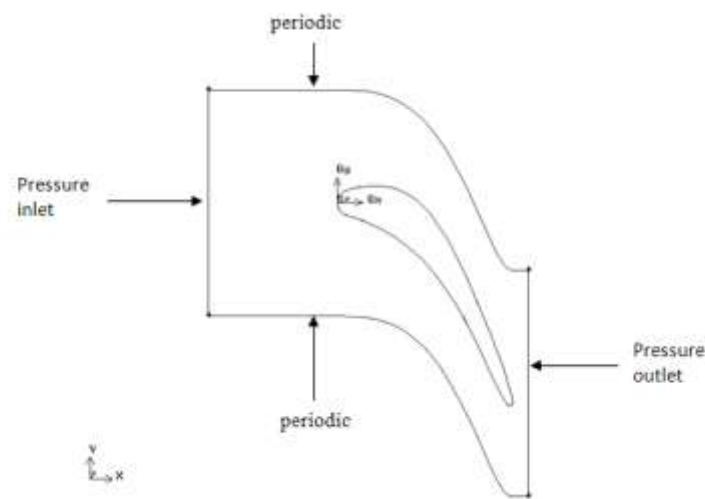


Figure 2. Boundary condition setup.

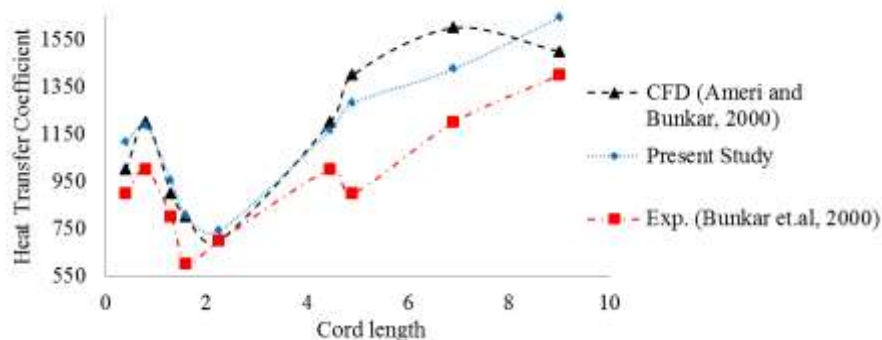


Figure 3. Comparison of heat transfer coefficient obtained in the present study with that of the previous workers.

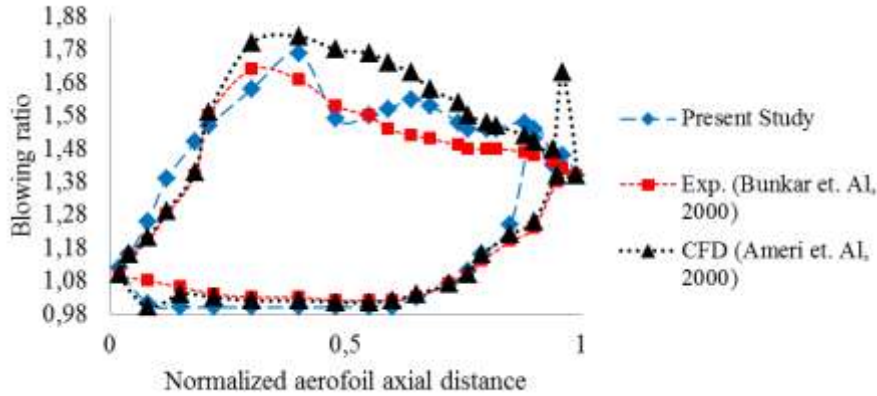


Figure 4. Pressure distribution around the blade at mid span (comparison of present prediction with previous works).

Temperature distribution

The contours of total temperature for the fluid layer generated by the film cooling around the blade surface, at the pressure and suction sides, in the case of four rows, are shown in Figure 5.

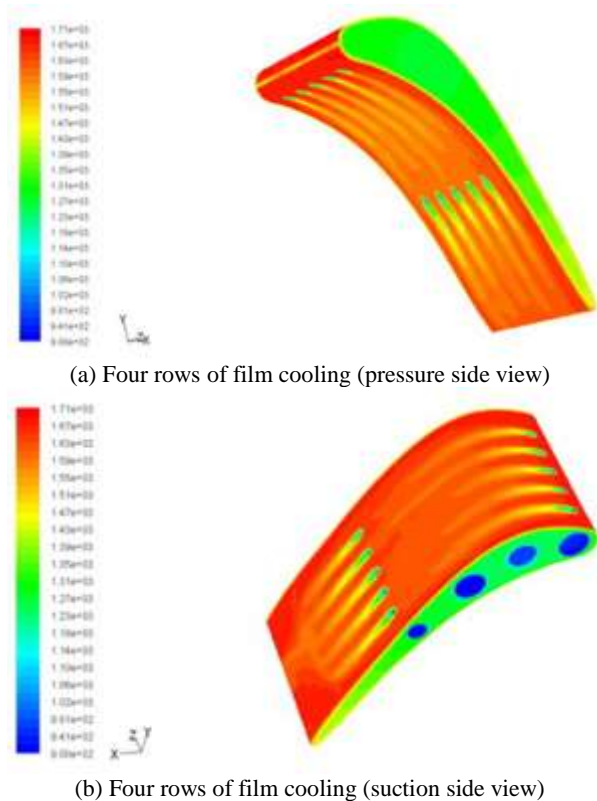


Figure 5. Predicted contours of total temperature on pressure and suction sides, with four rows film cooling.

The figure illustrates that the temperature varies around the blade surface. The trend of the fluid layer covering the blade surface predicts that the leading edge of blade surface has the highest temperature because of the stagnation flow and the film cooling hole regions are the coolest. The injection of the coolant with the use of the model is clearly seen. The flow is accelerating downstream of the holes because of the positive stream-

wise pressure gradient. However, the mainstream (hot gases) is impinged and turbulently mixed with the individual streams ejected out of the holes that are arranged at different orientations, and eventually spreads over the blade surface. Thus, due to the spraying of coolant on the blade surface the heat load on the surface of blade is removed systematically along the stream-wise direction.

Figure 6 shows the total temperature contours in the case of eight rows film cooling. All figures illustrate that the temperature varies around the blade surface. As in the previous case, the leading edge of blade surface has the highest temperature because of the stagnation flow and the film cooling hole regions are the coolest. It can be clearly seen that the downstream film holes arrangement covers a wider area of the blade surface than the hot gas flow arrangement. The downstream film holes arrangement has produced a better film cooling effectiveness since the film holes are located downstream of the leakage flow to protect more blade surface area. It is interesting to observe that in the area of highest blowing ratio near the pressure side of the leading edge, some of the jets appear to be lifting off, just as in the cylindrical passage. This seems to suggest that the lift-off in that region was not only due to high blowing ratios, but also because of strong secondary flows. Meanwhile, the holes near the suction side are swept towards the suction side following the near-wall streamlines, while the holes near the pressure side are directed along the path dictated by their orientation angles. The temperature predictions indicate that the blade with eight rows film cooling with internal channel is the best in terms of cooling performance.

Pressure and velocity distributions

As all the blade cases that are presented have the same aerofoil geometry with the same blowing ratio (P_{inlet}/P_{ex}) of 1.8, the pressure and velocity around the blade surface seems to be identical for all the cases. Hence, the static pressure and velocity are mentioned only for one case. Figure 7 shows the contours cross section of static pressure on the entire blade including the leading

edge region. It can be seen that the primary effect of the stagnation flow at the leading edge region is the highest pressure value. The analysis performed led us to the conclusion that the suction side has the lower pressure on the aerofoil surface, because of the acceleration flow on that region. The high pressure distributions are on the pressure side of the aerofoil surface, due to the low speed flow at the bottom of the aerofoil.

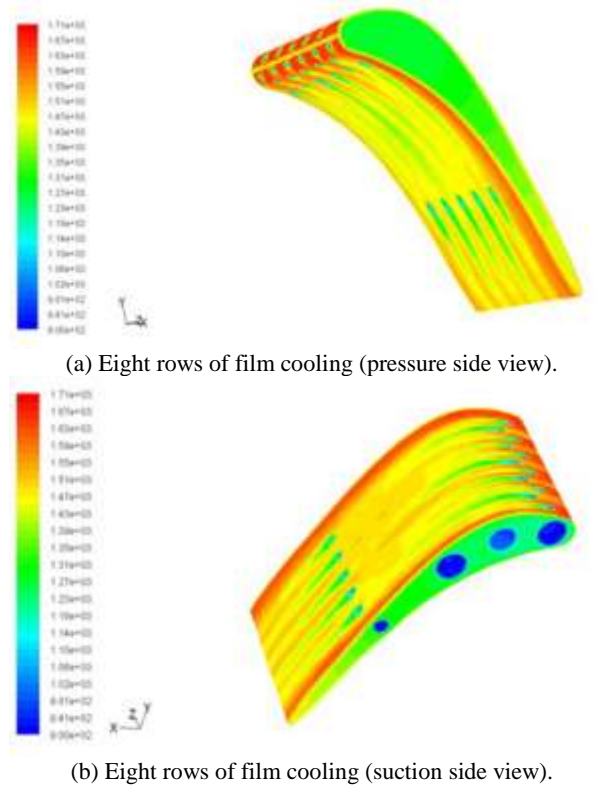


Figure 6. Predicted contours of total temperature on pressure and suction sides, with eight rows film cooling.

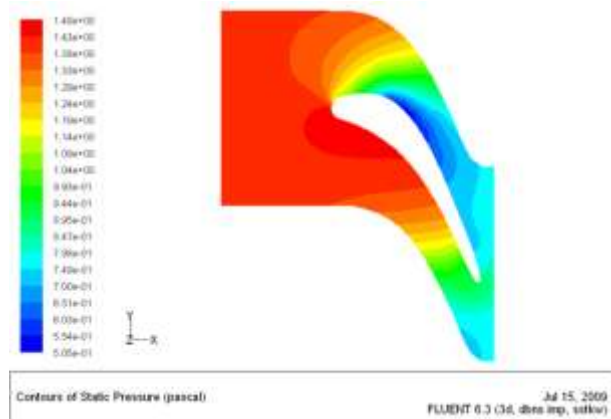


Figure 7. The static pressure contour around the blade.

As illustrated in Figure 7, the simulation blade model consists of one blade with two aerofoil-shaped passages on either side. At the leading edge of the blade (the stagnation point), the flow is divided and enter the passages. It is expected that, the similarity of flows in the passages is quickly lost as they approach the mid-chord of the blade because of the difference in blade surface profiles (convex at the suction side and concave at the pressure side). Figure 8 shows the contours of

pressure distribution at the mid-span of blade for suction and pressure sides. It can be seen clearly that the maximum value of static pressure is at the leading edge, due to the stagnation flow at this region. After the leading edge, the static pressure at the pressure side is observed to be higher than that at the suction side due to the accelerated flow at the suction side and retarded flow at the pressure side. It is worth noting that the region at the last quarter aft is suddenly dropping, due to the higher acceleration flow at this region.

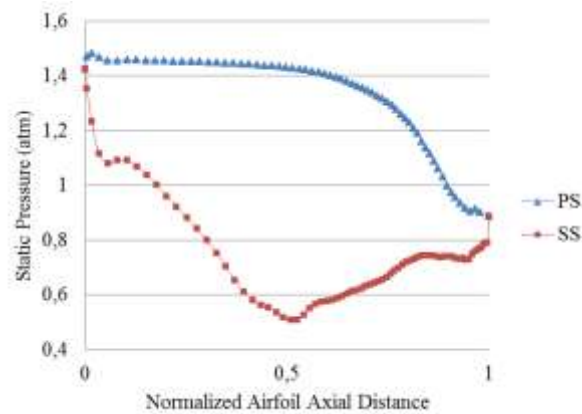


Figure 8. The static pressure curves around the blade.

In general, a lower value of static pressure corresponds to a higher local velocity, while a higher value corresponds to a lower local velocity. The present results of pressure agree well with those obtained by Ameri and Bunker (2000). Figure 9 shows the contours of airflow pattern in vertical plane for gas turbine blade plotted by velocity vector with blowing ratio (P_{in}/P_{ex}) of 1.8, when the hot gas is supplied with inlet temperature of 1700K. It may be observed that generally flow velocity is rather low on this plane except near the outlet and the suction side. The plane is clearly characterized by airflow caused by the moving hot gas from the combustion chamber to the turbine stage. The hot gas tends to flow from the inlet level downstream skirting the right hand side wall and, thereafter breaking into tow streams at the leading edge region, one stream moving towards the pressure side while the other stream moving to the suction side. The hot gas velocity is rather low resulting in stagnation zone at the leading edge. It is observed that the airflow is relatively stronger on the suction side of airfoil while the flow is lower on the pressure side. The hot gas is seen to be rushing from the trailing edge for both, suction and pressure sides.

Effect of coolant injection pressure ratio on temperature distribution

The temperature contours on the blade surface are plotted with three different coolant injection pressure ratios ($P_{R,ci} = \frac{P_{c,in}}{P_{c,ex}}$), 1.12, 1.30 and 1.45 at the same condition of downstream blowing ratio. For each case, the inlet velocity of downstream is 140 m/s at 1700 K with turbulent intensity 9% and blowing ratio 1.87. The

coolant injection temperature is kept at 900 K and the total coolant inlet pressure is varied as 1.6, 1.8 and 2 atm respectively. Figure 10 illustrates the effect of coolant injection pressure ratio ($P_{R,ci}$) on the temperature distribution of gas turbine blade surface. Generally, the temperatures are reduced significantly with the increase in the coolant injection for all film cooling tube area that is connected with a circular plenum.

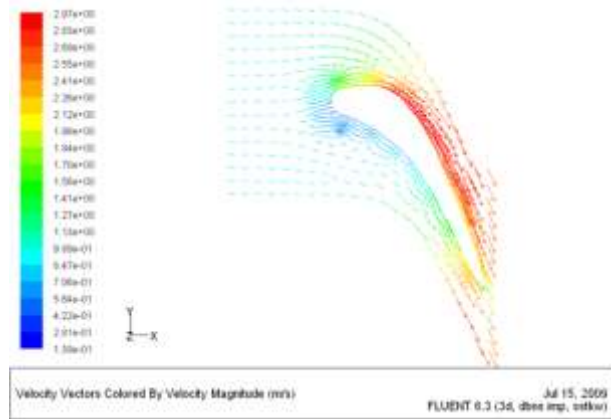


Figure 9. Velocity vector around the blade surface.

The jets are lifted off initially, but at downstream they impinge on the blade surface, which causes lateral spreading. The rows of film cooling holes show lift-off by a narrowing in the jet contour just downstream of the hole-exit. However, near the downstream the jets begin to spread laterally. It is interesting to note that lateral spreading zone increases with increase in the coolant injection pressure ratio. Figure 11 shows the zooming of film cooling hole plotted at three coolant injection pressure ratios ($P_{R,ci}$); the effect of injection cooling can be seen clearly. In general, the increase in $P_{R,ci}$ has led to reduction in the temperature and moreover the lateral spreading facilitated the best coolant layer.

Heat transfer coefficient

In this analysis, it is understood that the heat transfer coefficient is a function of the fluid flow field and independent of the temperatures of the blade and fluid. In order to find out the pure film cooling performance without the complication caused by the turbine work process, it is desirable to calculate another case for the same flow condition in the absence of film coolant injection. This enables us to determine the true effect of

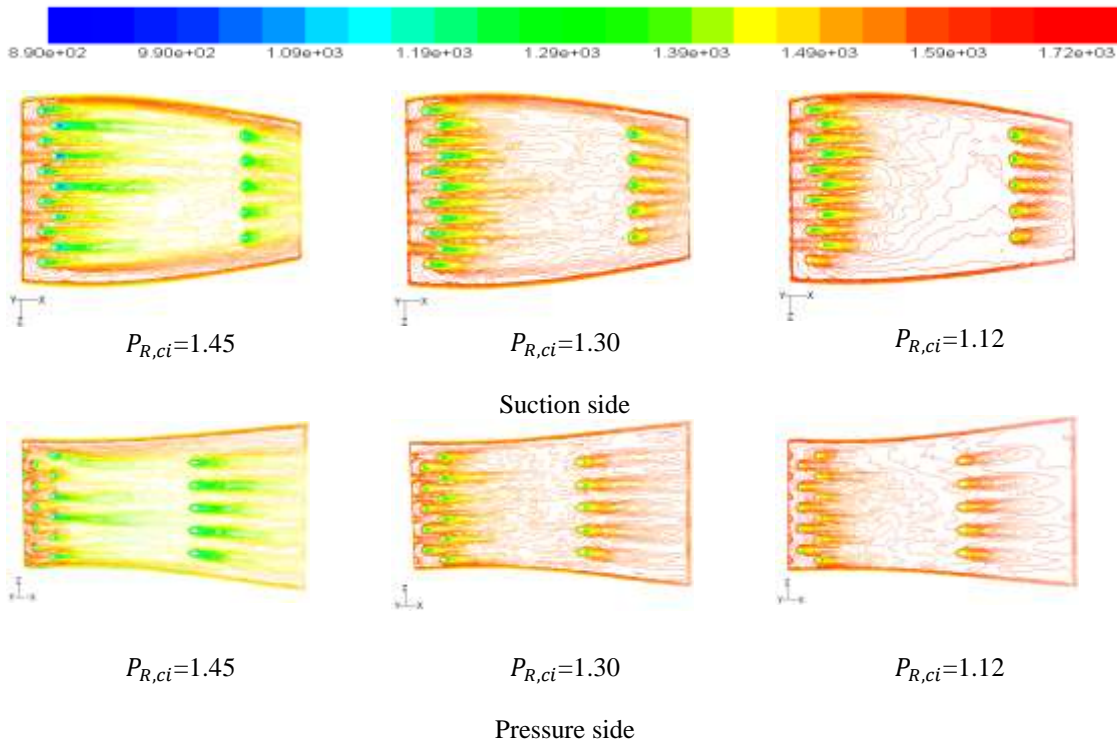


Figure 10. Temperature contours showing the effect of coolant injection pressure ratio.

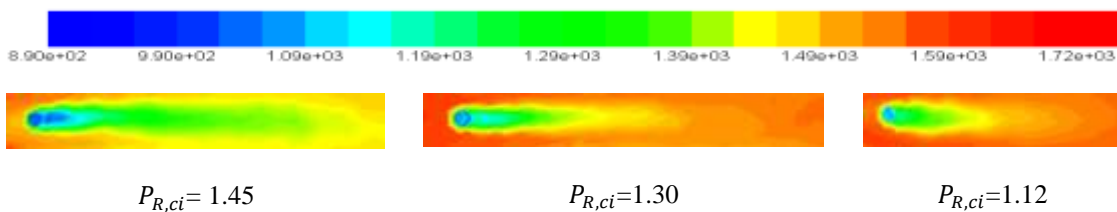


Figure 11. Zoomed temperature contours for three different coolant injection pressure ratios.

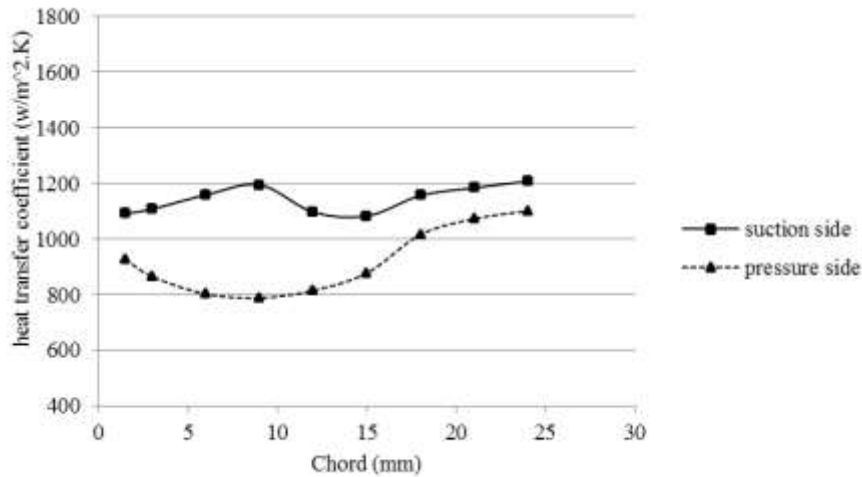


Figure 12. Heat transfer coefficient without film cooling.

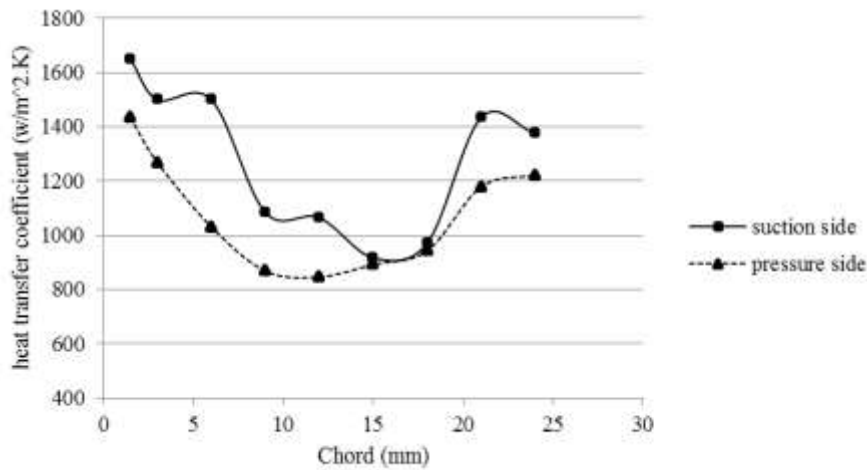


Figure 13. Heat transfer coefficient with film cooling.

coolant protection by comparing the temperature differences between the two cases (with and without the presence of film coolant). The thermal conductivity k is taken as 33w/m.K , inlet temperature 1700 K , blowing ratio ($P_{t,in}/P_{ex}$) 1.8 and turbulent intensity 9% . Figures 12 and 13 show the steady state heat transfer coefficients at suction and pressure sides at the design condition, without and with film cooling, respectively.

It is observed that heat transfer coefficient of the blade with one U-bend cooling channel is lower than that of the blade of eight rows film cooling with external channel, due to the effect of film cooling. In both cases, it is clear that the high heat transfer exists at the suction side due to high velocity, while low heat transfer happens at the pressure side because of the low velocity. Also the coolant jet significantly increases the intensity of unsteady heat transfer coefficient, because it disturbs the mainstream flow on impingement with the coolant flow at the blade surface. The effect of this kind by coolant is significantly high on the suction side, since the flow meets the positive pressure gradient there, and tends to be more easily disturbed. At the leading edge region of the blade, the heat transfer is further enhanced downstream of the film holes by coolant jets which

disturbs the mainstream flow. The heat transfer coefficient is higher near the trailing edge in comparison with that observed near the mid-chord region. Further, a region of high heat transfer coefficient is observed along the suction side. The average heat transfer coefficients are 1030.61 and $1176.71\text{ W/m}^2.\text{K}$ for the blade without and with film cooling respectively. It may be concluded that the blade with eight rows film cooling and internal channel is found to possess the highest heat transfer coefficient and hence the cooling performance.

CONCLUSION

The gas turbine blade performance with film cooling is investigated by CFD simulations using FVM. Normally, the turbine blade surface including suction side, pressure side and leading edge, experience a high heat load. Numerical investigations have been applied on the flow and film cooling for these critical regions. Generally, the predicted pressure and heat transfer coefficient agree well with the previous numerical and experimental data, with slight over-prediction in case of film cooling. For the combined internal and film cooling, two cases namely, the eight rows film cooling with internal U-bend channel and the four rows film

cooling with internal U-bend channel are presented. The temperature on the blade fluid surface decreases with increase in the number of film cooling holes, consequently the best cooling performance is observed by the eight rows film cooling with internal U-bend channel model. The heat transfer coefficients with and without film cooling are also compared. It has been predicted that the highest heat transfer coefficient is for the film cooling technique. However, in both cases, the heat transfer coefficient on the suction side was significantly higher than that at the pressure side. As future work, the present simulation results may be substantiated by adequate experiments.

REFERENCES

Abuaf, N., Bunker, R., Lee, C. P., Heat transfer and film cooling effectiveness in a linear airfoil cascade, *Journal of Turbo machinery (Transactions of the ASME)*, 119, 302-309, 1997.

Ahn, J., Mhetras, S., Han, J.-C., Film-Cooling effectiveness on a gas turbine blade tip using pressure-sensitive paint, *Journal of Turbo machinery (Transactions of the ASME)*, 127, 521-530, 2005.

Ahn, J., Schobeiri, M., T., Han, J. -C., Moon, H.-K., Film cooling effectiveness on the leading edge region of a rotating turbine blade with two rows of film cooling holes using pressure sensitive paint, *ASME Journal of Heat Transfer*, 128, 879-888, 2006.

Ahn, J., Schobeiri, M.T., Han, J.-C., Moon, H-K., Effect of rotation on leading edge region film cooling of a gas turbine blade with three rows of film cooling holes, *International Journal of Heat and Mass Transfer*, 50, 15-25, 2007.

Ameri, A. A., Bunker, R. S., Heat Transfer and Flow on the First-Stage Blade Tip of a Power Generation Gas Turbine: Part 2—Simulation Results, *Journal of Turbo machinery (Transactions of the ASME)*, 122, 272-277, 2000.

Bunker, R.S., Bailey, J.C., Ameri, A.A., Heat transfer and flow on the first-stage blade tip of a power generation gas turbine: Part 1—Experimental Results, *Journal of Turbo machinery (Transactions of the ASME)*, 122, 263-271, 2000.

Burdet, A., Abhari, R., S., Three-dimensional flow prediction and improvement of holes arrangement of a film-cooled turbine blade using a feature-based jet model, *Journal of Turbo machinery (Transactions of the ASME)*, 129, 258-268, 2007.

Chernobrovkin, A., Lakshminarayana, B., 1999. Numerical simulation and aerothermal physics of leading edge film cooling, *Proc. IMechE Part A: J. Power and Energy*, 213:103-118, 1999.

Choi J.-h., Mhetras S., Han J.-C., Lau S.C., Rudolph R., Film cooling and heat transfer on two cutback trailing edge models with internal perforated blockages, *Journal of Turbo machinery (Transactions of the ASME)*, 130, 012201-012213, 2008

Fluent Inc., Version 6.0, 2002 CD-ROM, Fluent Inc, Lebanon, New Hampshire.

Gao, Z., Narzary, D.P., Han, J.-C., Film cooling on a gas turbine blade pressure side or suction side with axial shaped holes, *International Journal of Heat and Mass Transfer*, doi:10.1016/j.ijheatmasstransfer.2007.11.010 in press, 2007.

Gao Z., Narzary D.P., Han J-C., Film-Cooling on a gas turbine blade pressure side or suction side with compound angle shaped holes, *Journal of Turbo machinery (Transactions of the ASME)*, 131, 0110191-11, 2009.

Heidmann, J.D., Rigby, D.L., Ameri, A.A., A three-dimensional coupled internal/external simulation of a film-cooled turbine vane, *Journal of Turbo machinery (Transactions of the ASME)*, 122, 348- 359, 2000.

Heidmann, J., D., Lucci, B., L., Reshotko, E., An experimental study of the effect of wake passing on turbine blade film cooling, *Journal of Turbo machinery (Transactions of the ASME)*, 123, 214-221, 2001.

Kwak, J.S., Han, J.-C., Heat Transfer Coefficients and Film-Cooling Effectiveness on a Gas Turbine Blade Tip, *Journal of Turbo machinery (Transactions of the ASME)*, 125, 494-502, 2003a.

Kwak, J.S., Han, J.C., Heat transfer coefficients and film cooling effectiveness on the squealer tip of a gas turbine blade, *Journal of Turbo machinery (Transactions of the ASME)*, 125, 648- 657, 2003b.

Kwak, J.S., Ahn, J., Han, J.C., Lee, C. P., Bunker, R.S., Boyle, R., Gaugler, R., Heat transfer coefficients on the squealer tip and near-tip regions of a gas turbine blade with single or double squealer, *Journal of Turbo machinery (Transactions of the ASME)*, 125, 717- 779, 2003.

Kwak, J.S., Han, J.C., Heat transfer coefficients on the squealer tip and near squealer tip regions of a gas turbine blade, *Journal of Turbo machinery (Transactions of the ASME)*, 125, 669- 667, 2003c.

Martini, P., Schulz, A., Whitney, C. F., Lutum, E., 2003. Experimental and numerical investigation of trailing edge film cooling downstream of a slot with internal rib arrays, *Proc. IMechE Part A: J. Power and Energy*, 217: 393-401, 2003.

McDonnell Douglas A-4 Skyhawk available at: http://en.wikipedia.org/wiki/Douglas_A-4_Skyhawk.

Menter, F., R., Two-Equation Eddy-Viscosity Turbulence Models for Engineering Applications, *AIAA Journal*, 328.1598-1605, 1994.

Montomoli, F., Adami, P., Martelli, F., 2009. A finite-volume method for the conjugate heat transfer in film cooling devices, *Proc. IMechE Part A: J. Power and Energy*, 223: 191-200, 2009.

Sarkar, S., Das K., Basu, D., 2001. Film cooling on a turbine guide vane: a numerical analysis with a multi-grid technique, *Proc. IMechE Part A: J. Power and Energy*, 215: 39-53, 2001.

Scheepers, G., Morris, R., M., Experimental study of heat transfer augmentation near the entrance to a film cooling hole in a turbine blade cooling passage, *Journal of Turbo machinery (Transactions of the ASME)*, 131, 044501-1-044501-11, 2009.

Tao, Z., Zhao, Z., Ding, S., Xu, G., WU, H., Suitability of three different two-equation turbulence models in predicting film cooling performance over a rotating blade, *International Journal of Heat and Mass Transfer*, 52 5-6, 1268–1275, 2009.

Teng S., Sohn D.K., Han J.-C., Unsteady wake effect on film temperature and effectiveness distributions for a gas turbine blade, *Journal of Turbo machinery (Transactions of the ASME)*, 122, 340 – 347, 2000.

Yang, C., S., Lin, C., L., Gau, C., Film cooling performance and heat transfer over an inclined film-cooled surface at different convergent angles with respect to highly turbulent mainstream, *International Journal of Heat and Mass Transfer*, 29, 167-177, 2009.

Yang, H., Chen, H.-C., Han, J.-C., Moon, H.-K., Numerical study of film cooled rotor leading edge with tip clearance in 1-1/2 turbine stage, *International Journal of Heat and Mass Transfer*, doi:10.1016/j.ijheatmasstransfer.2007.09.025., 2007.